

Aggregation kinetics and stability of structures formed by magnetic microspheres

Weijia Wen,¹ F. Kun,^{2,*} K. F. Pál,³ D. W. Zheng,¹ and K. N. Tu¹

¹Department of Materials Sciences and Engineering, UCLA, Los Angeles, California 90095-1595

²Institute for Computer Applications (ICA1), University of Stuttgart, D-70569 Stuttgart, Germany

³Institute of Nuclear Research (ATOMKI), P.O. Box 51, H-4001 Debrecen, Hungary

(Received 5 November 1998)

Stable rings formed by magnetization-controllable microspheres at zero field are observed and reported in this Rapid Communication. The magnetic microspheres were made by plating glass beads with a critical thickness of Ni film. We found that the ring leading to magnetic flux closure is the most stable configuration. At high concentrations, all individual rings, chains, and clusters join together to form a netlike structure. A computer simulation based on the dipole-dipole interaction, without thermal noise, has been carried out, and the results are in good agreement with the experimental observations. Based on an analytic approach we give a simple explanation of the formation and stability of rings. [S1063-651X(99)50105-0]

PACS number(s): 83.10.Pp, 82.70.Dd, 61.43.Hv

The spatial configurations of magnetic microspheres in colloid and complex fluids is an interesting issue concerning the magnetic materials, nonlinear science, and fundamental statistical mechanics. As early as the 1970's, de Gennes and Pincus [1] predicted that without a magnetic field the magnetic particles suspended in a passive liquid form randomly oriented *chains* competing with closed *rings* and *clusters*. Under an external field H , they change to *chains* along the field direction. Although some preliminary investigations have been carried out [2–5], no direct evidence supporting the prediction has been reported to date. The effect of long range dipolar forces on the dynamics of growth processes and on the structure of growing aggregates in colloids has been extensively studied in the framework of particle-cluster aggregation [6] and cluster-cluster aggregation [5], but the interesting effect of ring formation and competition of closed rings with open chains has not been observed.

For the purpose of the experiments, we fabricated magnetization-controllable microspheres by coating uniform-size glass beads with a nickel layer of given thickness. By using such microspheres we could study the pattern formation in two dimensions, and we found that the features of pattern formation are in good agreement with the theoretical predictions of de Gennes and Pincus [1]. We observed that (a) microspheres prefer to form isolated rings in low concentrations and change to cluster or netlike structure in high concentrations, (b) rings leading to magnetic flux closure are the most stable configurations. A two-dimensional dynamic simulation, based on the dipole-dipole interaction without thermal noise, has been carried out to support the observations. Based on the simulation and the analytic investigation of stability of aggregates we could draw interesting conclusions on the aggregation kinetic and ground state conformation of the ensemble of magnetic microspheres in the absence of annealed disorder.

In order to obtain moment-controllable spherical particles, we selected uniform glass microspheres with average diam-

eters of $47\ \mu\text{m}$ as an initial core and coated a thin layer of nickel using electroless plating [7]. We found that, for microspheres with a moderate value of magnetic moments, the optimum thickness of nickel ranges from 2.5 to $4\ \mu\text{m}$. The magnetization of microspheres used in our experiment is about $1.56\ \text{emu}/\text{cm}^3$, which can be calculated by multiplying the volume of the nickel shell with the saturation magnetization of nickel at $480\ \text{emu}/\text{cm}^3$ [8]. The dimensionless parameter K_{dd} , characterizing the strength of the magnetic coupling relative to the thermal energy, is

$$K_{dd} = \frac{\mu^2}{d^3 k_B T} = \frac{\pi^2}{36} \frac{M^2 d^3}{k_B T}. \quad (1)$$

Hence, at a fixed ambient temperature T the value of K_{dd} can be controlled by adjusting either the magnetization M or the diameter d of the particles. Here, the value of K_{dd} is about 1.69×10^6 . In the experiments the optical side of a six inch Si wafer was used as the bottom plate on which four plastic barriers are mounted to form a container filled with alcohol or oil. The pattern evolution of microspheres in the container was monitored *in situ* by a charge-coupled device (CCD) camera and a video recorder. First, the nickel-coated microspheres were magnetized inside an electromagnet and then dispersed randomly onto the container as seen in Fig. 1(a), where some short chains coexisted with a few rings and clusters. Due to the relatively large particle size, this state remained unchanged if there was no external perturbation. After we perturbed the system by slightly vibrating the wafer to overcome the frictional barrier, individual microspheres, short chains, and small clusters began to move and form longer chains or longer clusters. Simultaneously, some chains or clusters closed themselves to form rings [see Fig. 1(b)]. The final pattern is exhibited in Fig. 1(c), where almost all rings and clusters joined together to form a netlike structure. It has to be noted that comparing our experimental results to ones known in the literature [5], the main difference is that our aggregates do not have ramified structure, i.e., the chains and rings have regular shapes. The absence of the Brownian effect in our case is due to the much larger particle

*Permanent address: Department of Theoretical Physics, Kossuth Lajos University, P.O. Box 5, H-4010, Debrecen, Hungary.

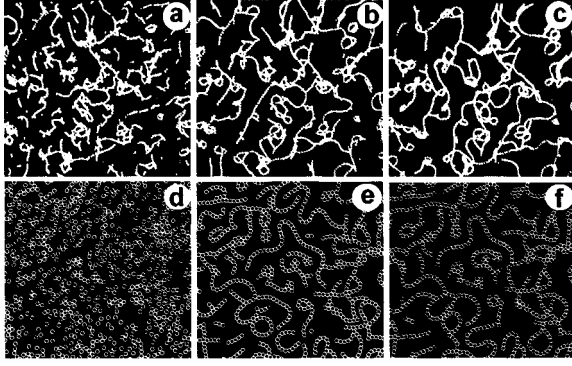


FIG. 1. (a)–(c) show the evolution of the ring, chain, and cluster formed by the magnetic microspheres dispersed on the silicon wafer under slight vibration. (d)–(f) show the time evolution of the aggregation process obtained by computer simulation.

size compared to Ref. [5]. The relatively larger particle size hinders the Brownian motion and it also results in a larger value of dipole moment μ leading to stronger magnetic coupling (i.e., large K_{dd}) at a moderate level of magnetization M . The Brownian motion of small size particles and the polarization, due to the higher level of magnetization in Ref. [5], seem to be the main reasons why it is impossible to observe the competition of regularly shaped rings and chains there.

To support the above argument and to gain deeper insight into the aggregation process, we have studied the pattern formation in the absence of an external magnetic field also by computer simulation. In the simulation, the system under consideration is modeled as the monodisperse suspension of nonBrownian soft particles of number N with diameter d and magnetic moment μ [$\mu = M(\pi d^3/6)$]. The particles are represented by moving spheres in a two-dimensional plane.

The time evolution of the system is followed by solving the equations of motion for the translational degrees of freedom of the particles (molecular dynamics [9]) and followed by applying a relaxation technique to also capture the rotation of the dipoles. The particles are subjected to dipole-dipole interaction, to hydrodynamic resistance due to their motion relative to the liquid phase, and to an elastic restoring force (soft particle dynamics) in order to take into account the finite size of the particles. The magnetic force \vec{F}_{ij}^m , acting between two dipoles $\mu\vec{e}_i$ and $\mu\vec{e}_j$, separated by distance r_{ij} , is

$$\begin{aligned} \vec{F}_{ij}^m &= \mu^2 \frac{3}{r_{ij}^4} [5 \cos \beta_i \cos \beta_j \vec{n}_{ij} - \cos(\beta_i - \beta_j) \vec{n}_{ij} \\ &\quad - \vec{e}_i \cos \beta_j - \vec{e}_j \cos \beta_i] \\ &= \mu^2 \vec{f}_{ij}^m, \end{aligned} \quad (2)$$

where \vec{n}_{ij} denotes the unit vector pointing from dipole i to dipole j , and β_i , β_j are the angles of the direction of the dipoles with respect to \vec{n}_{ij} . The hydrodynamic force $\vec{F}_{ij}^{\text{hyd}}$ on a sphere is treated as Stokes's drag

$$\vec{F}_i^{\text{hyd}} = -\alpha \vec{v}_i, \quad (3)$$

where the parameter α depends on the particle size and viscosity of the fluid, and $\vec{v}_i = d\vec{r}_i/dt$ denotes the velocity of particle i . In order to take into account the finite size of the particles we apply the so-called soft particle dynamics, i.e., the particles are allowed to overlap each other up to some extent during their motion. We introduce the elastic restoring force $\vec{F}_{ij}^{\text{cont}}$ (contact force) between the overlapping particles according to the Herz contact law [10]

$$\vec{F}_{ij}^{\text{cont}} = -k(d - r_{ij})^{3/2} \cdot \vec{n}_{ij} = -k\vec{f}_{ij}^{\text{cont}}, \quad (4)$$

where k is a material dependent constant. For simplicity, in the simulations the system is supposed to be fully dissipative, noninertial. Hence,

$$\frac{d\vec{r}_i}{dt} = \frac{\mu^2}{\alpha} \sum_j \vec{f}_{ij}^m - \frac{k}{\alpha} \sum_{r_{ij} < 2R} \vec{f}_{ij}^{\text{cont}}, \quad i = 1, \dots, N, \quad (5)$$

the first order differential equation system is solved numerically to obtain the trajectory of the particles [9], starting from a random spatial configuration. Motivated by the experimental observations, the equation of the motion [Eq. (5)] does not contain a stochastic component, i.e., randomness is introduced into the model solely through the random initialization of position of the particles and the direction of their dipole moments (quenched disorder). This implies that the simulation corresponds to the case $K_{dd} = \infty$ and, hence, the trajectory of particles is determined. Without loss of generality, the parameter values used in the simulations are $\mu^2/\alpha = 1$ and k/α were chosen such that the overlap of the contacting particles is always much smaller than d . The rotation of the particles due to the dipole-dipole interaction is not dynamically implemented. Instead, after each integration step of Eq. (5), a self-consistent relaxation algorithm is used to find the equilibrium orientation of dipoles where no torque acts on them anymore. The periodic boundary condition is used in both directions in the two-dimensional simulation. The simulation results can be seen in Figs. 1(d)–1(f). Comparing the patterns presented in Fig. 1, it can be seen that the simulation results are in good agreement with the experimental ones, which justifies that the dipolar interaction is already sufficient for the occurrence of phenomena.

Figure 2 displays the effects of concentration of microsphere per unit area on the patterns. In low concentrations, most microspheres form isolated rings [Fig. 2(a)]. When the concentration is increased, individual rings, connected rings, and clusters appeared simultaneously [see Fig. 2(b)]. However, if the concentration was increased to a certain value, all rings and chains connected to form closed clusters or netlike structures. In this case, almost no individual ring was observed [see Fig. 2(c)]. The simulation results performed with different concentrations are shown in Figs. 2(d)–2(f), where again the good agreement between theory and experiments can be seen.

It is easy to show by analytic means that the deepest energy confirmation of dipoles is a ring, whenever the number of dipoles exceeds three [11,12]. In spite of this, the formation of rings in a suspension is not obvious to understand, especially in the absence of annealed disorder, since the dipolar interaction tries to locally align the dipole moments. To obtain information about the chain-ring transition and the

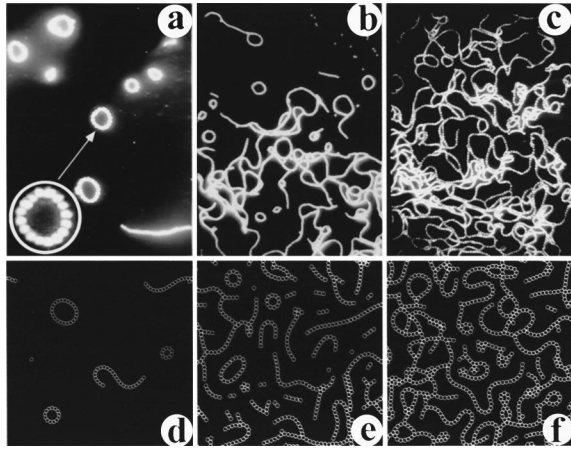


FIG. 2. Patterns formed at different concentrations. Here, the concentrations for (a), (b), and (c) are 1.89, 20.08, and 42.95 %, respectively. (d)–(f) show the results of the computer simulations of the corresponding systems.

stability of these structures, we calculated analytically how the energy of a chain of N dipoles changes when the chain is gradually bent and finally closed to create a ring. The gradual deformation of a chain is performed in such a way that the particles are always constrained onto a circle characterized by an angle γ , the value of which varies between 0 (straight chain) and 2π (closed ring). It is supposed that during the deformation the dipole moments point into the direction of the local tangent of a circle. Summing over all the possible pairs of dipoles, the energy per particle $w_N(\gamma)$ of a deformed chain of N elements as a function of γ can be cast into the form

$$w_N(\gamma) = -\frac{\mu^2 \sin^3(\gamma/2N)}{Nd^3} \sum_{i=1}^{N-1} \frac{1 + \cos^2(i\gamma/2N)}{\sin^3(i\gamma/2N)} (N-i). \quad (6)$$

In Fig. 3, $w_N(\gamma)$ is plotted as a function of γ for several values of N . Note that the limiting cases $\gamma \rightarrow 0$ and $\gamma \rightarrow 2\pi$ of Eq. (6) give the energy of a straight chain and of a perfect ring

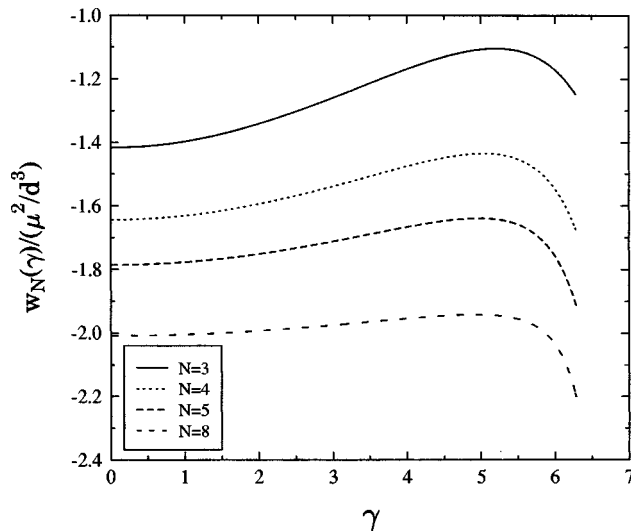


FIG. 3. The dimensionless ratio $w_N(\gamma)$ and μ^2/d^3 for four different values of N . γ varies between 0 and 2π .

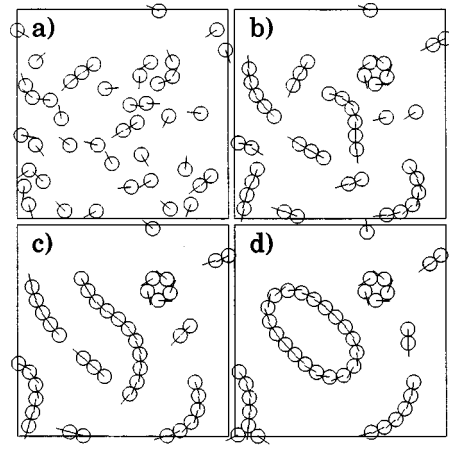


FIG. 4. Magnified view of a region of the suspension where rings of 5 and 19 dipoles appear. The four snapshots of the simulation show the aggregation process leading to the formation of magnetic rings.

ring, respectively. It can be observed in Fig. 3 that, for $N > 3$, the ring configuration has the deepest energy. The minima of $w_N(\gamma)$ corresponding to the straight chain and the perfect ring configurations are separated by a maximum w_N^{\max} with a position γ_N^{\max} .

The chains have a certain rigidity against bending, since, in the bent chain, the dipoles are not in the energetically favorable fully aligned configuration anymore. However, when the bending angle exceeds the threshold value γ_N^{\max} , the energy starts to decrease again, and the closing of the chain becomes favorable. This is due to the attraction of two ends that are close to each other. This has important consequences on the mechanism of the ring formation. A ring cannot be formed from a single chain. One has to overcome a broad potential barrier to bend the chain until it will close. Also, a single chain tends to grow longer along a straight line until there are mobile single balls or very short chains around its ends. Therefore, a ring can only form from two or more open chains of appropriate relative position, direction, and polarization. It is not difficult to see that the emergence of such chains is not purely due to the disorder present; it is encouraged by the closed loops of the magnetic field lines. The aggregation process of chains leading to the creation of two rings is demonstrated in Fig. 4. At the beginning of process, the dipoles that happen to be very close to each other in initial random configuration align and stick together forming pairs and short chains. While their magnetic field makes single dipoles around their ends align them, it forces nearby dipoles in the perpendicular direction from them to take the opposite polarization. This way, chains of one polarization encourage the formation of parallel chains of opposite polarization. One can see in Fig. 4(a) that parallel short chains just being formed really tend to be polarized more or less oppositely. Such parallel chains attract each other, and they may soon form small rings [e.g., the ring with five particles in Figs. 4(a)–4(c)], or grow longer before their ends join. The ends may get closer to each other not only by the attractive force, but also by bridges built from more mobile short chains, which are moved by the magnetic field between the ends to fill the gap. The above argument also

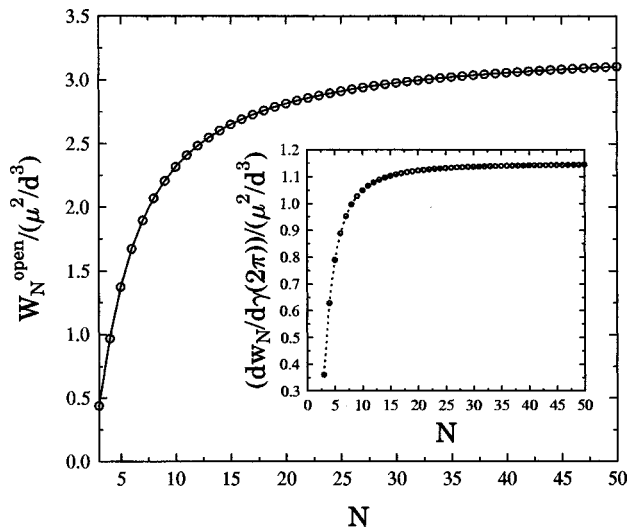


FIG. 5. W_N^{open} divided by μ^2/d^3 as a function of N . The inset shows $dw_N/d\gamma$ divided by μ^2/d^3 at $\gamma=2\pi$ vs N obtained from Eq. (6).

implies that the ground state of the system is in ring configuration in the limit of small concentrations, while at larger concentrations, the chains may freeze in the local energy minimal forming branching cluster instead of rings.

To quantify the stability of rings, from Eq. (6) we calculated the total energy W_N^{open} required to open up a ring of N dipoles $W_N^{\text{open}} = N[w_N^{\text{max}} - w_N(2\pi)]$, i.e., the deepness of energy valley of rings in Fig. 3 multiplied by N . It can be observed in Fig. 5 that W_N^{open} is an increasing function of N and it tends to a limiting value for large N . Another characteristic quantity of the stability of rings is the force F that has to be exerted for the opening.

It can be shown that, in the vicinity of the bending angle $\gamma=2\pi$, the opening force F is proportional to the derivative

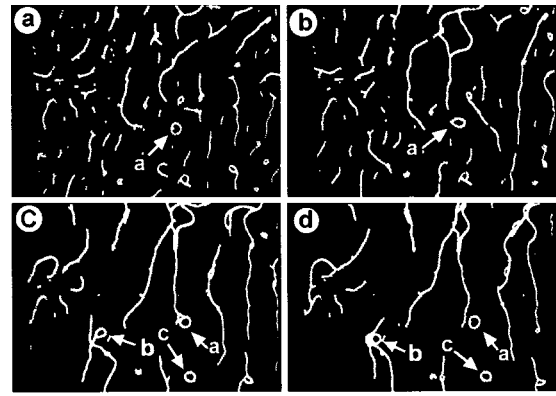


FIG. 6. Investigating the ring's stability under strong vibration by using a mechanic shaker.

of $w_N(\gamma)$ with respect to γ . In the inset of Fig. 5 one can observe that the derivative $dw_N/d\gamma$ at $\gamma=2\pi$ shows qualitatively the same behavior as W_N^{open} , i.e., the opening force F also saturates for large N . It has to be emphasized that the above analytic results cannot be obtained in the framework of the simple model of Ref. [12] where only the nearest neighbor interaction was taken into account, neglecting the important long range interaction of dipoles. The stability of the rings has been tested experimentally, which is shown in Fig. 6, where the system was subjected to strong vibrations on a mechanic shaker. In Fig. 6, we marked rings as a , b , and c , and then traced their whole trajectories under the vibration. The rings were very stable during the entire process, while the morphologies of the neighboring chains changed rapidly.

F. Kun is very grateful for the financial support of the SOROS Foundation. He also acknowledges financial support from OTKA T-023844.

-
- [1] P. G. De Gennes and P. A. Pincus, *Phys. Kondens. Mater.* **11**, 189 (1970).
 [2] R. E. Rosensweig, *Ferrohydrodynamic* (Cambridge University Press, New York, 1985).
 [3] S. Jin, T. H. Tiefel, R. Wolfe, R. C. Sherwood, and J. J. Motz, Jr., *Science* **255**, 446 (1992).
 [4] J. Liu, E. M. Lawrence, A. Wu, M. L. Ivey, G. A. Flores, K. Javier, J. Bibette, and J. Richard, *Phys. Rev. Lett.* **74**, 2828 (1995); J. Liu and M. Hagenbuchle, *Appl. Opt.* **36**, 7664 (1997).
 [5] A. T. Skjeltorp, *Phys. Rev. Lett.* **51**, 2306 (1983); G. Helgesen, A. T. Skjeltorp, P. M. Mors, R. Botet, and R. Jullien, *ibid.* **61**, 1736 (1988); G. Helgesen and A. T. Skjeltorp, *J. Appl. Phys.* **69**, 8277 (1991).
 [6] R. Pastor-Satorras and J. M. Rubi, *Phys. Rev. E* **51**, 5994 (1995); N. Vandewelle and M. Ausloos, *ibid.* **51**, 597 (1995).
 [7] W. Y. Tam, G. Yi, W. Wen, H. Ma, M. M. Y. Loy, and P. Sheng, *Phys. Rev. Lett.* **78**, 2987 (1997); W. Wen and K. Lu, *Phys. Fluids* **9**, 1826 (1997).
 [8] D. C. Jiles, *Introduction to Magnetism and Magnetic Materials* (Chapman and Hall, London, 1991).
 [9] M. P. Allen and D. J. Tildesley, *Computer Simulation of Liquids* (Clarendon, Oxford, 1994).
 [10] S. Luding, in *Collisions and Contact Between Two Particles*, Vol. 350 of *Physics of Dry Granular Media*, NATO Advanced Study Institute, Series E, edited by H. J. Herrmann, J.-P. Hovi, and S. Luding (Kluwer, Dordrecht, 1998).
 [11] I. Jacobs and C. Bean, *Phys. Rev.* **100**, 1061 (1955).
 [12] P. Jund, S. G. Kim, D. Tománek, and J. Hetherington, *Phys. Rev. Lett.* **74**, 3049 (1995).